Sensors & Actuators: A. Physical 339 (2022) 113506

Contents lists available at ScienceDirect

Sensors and Actuators: A. Physical

journal homepage: www.journals.elsevier.com/sensors-and-actuators-a-physical

A wide bandwidth real-time MEMS optical power meter with high resolution and linearity

Xuan Chen [a], Hairong Wang [a], Xueyong Wei [a,b,*]

[a] State Key Laboratory for manufacturing Systems Engineering, Xi'an Jiaotong University, Xi'an 710049, People's Republic of China
[b] State Key Laboratory of Applied Optics, Changchun Institute of Optics, Fine Mechanics and Physics, Chinese Academy of Sciences, Changchun 130033, People's Republic of China

ARTICLE INFO

Keywords:
MEMS
Micromechanical resonator
Optical power meter
Sensors

ABSTRACT

This paper presents a new type of wide bandwidth real-time micromechanical optical power meter based on a micro silicon disk resonator. The resonant frequency of micromechanical resonator is ultrasensitive with its heat absorption, which is verified by both simulation and experiment, including the open-loop and closed-loop testings. The resonant frequency of both the elliptical mode and contour mode of the disk resonator will shift when lasers of 488 nm and 1550 nm with different power are irradiated. The detector shows different heat absorption efficiency depending on the wavelength of the measured optical signal. The heat absorption efficiency was tested with 488 nm and 1550 nm laser irradiation in our experiments. According to our closed-loop experiments, the resolution of our detector could reach 78 nW, and a high linearity of $R^2 = 0.99605$ for the 488 nm target optical signal.

1. Introduction

Optical power measurement technique is one of the most important techniques in areas such as optical communications, astronomical photometry and military [1]. Two detecting methods commonly used for optical power detection are photoelectric detection and thermal detection. Photoelectric detectors like photomultiplier tubes (PMT) and single-photon avalanche diodes (SPAD) are based on semiconductors with narrow bandgaps [2,3]. The dark current will increase as temperature increases because of thermally generated charge carriers [4]. This kind of detectors are usually able to achieve high precision, but the range of wavelength can be detected is limited by the characteristics of semiconductors [5]. Besides, photoelectric detectors require cooling environment, making the system bulky and expensive [6]. Those optical power meters using thermal effect of laser, include the pyroelectric type [7] and the calorimetry type [8,9]. They measure the amount of heat absorbed by the sensitive components [10]. This type of power meter can work in room temperature or even above and have no limitations in target wavelength. However, most of thermal detectors have difficulties in improving resolution or response time. High resolution thermal detectors are usually quite complex in structure, making them difficult to popularize [11,12]. What's more, thermal detectors with high resolution are quite narrow in detectable power range. Thus, a portable optical power meter with high accuracy, expanded dynamic range and capability to work in wide wavelength range is in urgent need at present.

Due to the increased demand of micro-machined optical power meter in many different areas, such as spectrometer, gas detector and remote temperature detector, MEMS-based optical power meter has aroused great attention [12]. For example, the bimaterial microcantilevers are often used for sensitive detection of optical power. The microcantilevers will bend when laser power irradiates due to the differential expansion coefficients of two materials [13,14]. The precision of the optical power meter based on bimaterial microcantilevers depends on the precision of the displacement measurement, making the reading device complicated and expensive. Another type of MEMS optical power meter is based on resonator. Most of resonant optical power meter is AlN or GaN resonator with a resonant frequency of hundreds of MHz or several GHz which leads to a high scale factor between optical power and resonant frequency [15–17]. Due to the characteristics of piezoelectric resonator, they usually cannot reach high frequency resolution. Besides, complex read-out electronics are often needed due to the high resonant frequency (GHz) to prevent strong electromagnetic interferences.

A new type of optical power meter based on a single crystal silicon (SCS) disk resonator is proposed in this work. The optical power meter

* Correspondence to: Xi'an Jiaotong University, 28 West Xianning Road, Xi'an, Shaanxi Province, 710049, People's Republic of China.
E-mail address: seanwei@mail.xjtu.edu.cn (X. Wei).

https://doi.org/10.1016/j.sna.2022.113506
Received 9 January 2022; Received in revised form 26 February 2022; Accepted 9 March 2022
Available online 17 March 2022

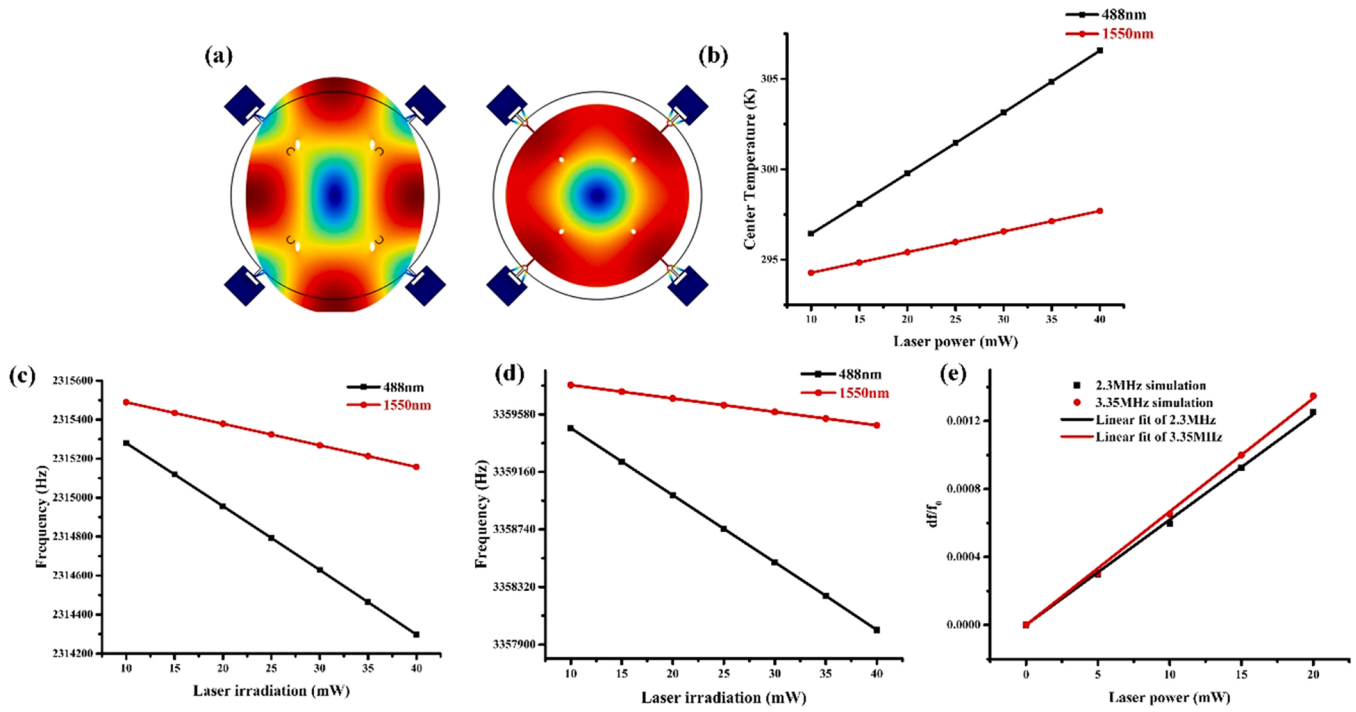

Fig. 1. (a) Elliptical mode (left) and the contour mode (right) shape of the resonator from Comsol® Multiphysics. (b) Computing the center temperature of the disk resonator at different laser power of 488 nm and 1550 nm, a linear relationship is concluded. (c) The frequency shift of the elliptical mode of the disk resonator when the laser power (both 488 nm and 1550 nm) increases from 10 mW to 40 mW. (d) The frequency shift of the contour mode of the disk resonator when the laser power (both 488 nm and 1550 nm) increases from 10 mW to 40 mW. (e) The scale factor between df/f_0 and laser power of the contour mode is slightly higher than it of the elliptical mode.

utilized frequency fluctuations of our resonator caused by laser induced heating. The temperature of the laser heated silicon is mainly determined by the intrinsic absorption of the semiconductor and the absorption on the thermal generated electron-hole pairs [18]. Thus, the optical power meter proposed by us is expected to be used in any range of optical spectrum. The good thermal conductance of silicon ensures a quick response time of our optical power meter. Due to the easy and sensitive detection of resonant frequency, our optical power meter can reach a detection limit of 78nW and realize real-time measurement with a less than 0.3 s response time. Besides, since silicon resonator has its unique advantages in integrating with electronics, our optical power meter is very promising for varied applications.

2. Design and simulation

The SCS optical power meter proposed by us is composed of three parts including a sensitive component, frequency tracking oscillator circuits and a monitor. The sensitive component of our detector is a SCS disk resonator. Different additive absorption materials can be applied to the surface of the resonator to increase the absorptivity of the power meter at a certain waveband. At present, gold and platinum are the most common absorptive materials [19,20]. Graphene layer is also used by some researchers on the aluminum nitride resonator [21,22]. The optical power meter proposed by us didn't use any absorption materials on our disk resonator due to the limitation of our microfabrication process. The frequency tracking oscillator circuits including an open-loop circuit and a closed-loop circuit shows the drift of the resonant frequency caused by temperature fluctuation. And the monitor shows the power of laser irradiation according to the correspondence between the resonant frequency and laser power.

The resonator used in this work is a SCS disk with a radius of 750 μm and a thickness of 10 μm. Comsol® Multiphysics was used to simulate the resonant mode and frequency of our disk resonator. Fig. 1(a) shows the elliptical mode (2.3 MHz) and the contour mode (3.36 MHz) of the disk resonator. Both two modes will be tested in following experiments. We also simulate the relationship between the resonant frequency and the laser power with 488 nm and 1550 nm. The simulation process is divided into two parts. First, the temperature distribution of the resonator is obtained according to the laser irradiation and the structure of resonator. A light beam with different wavelengths is modeled by the ray optics module in COMSOL. The light beam is set with a divergence angle of 0.2 rad, releasing from 2 mm off the resonator surface. Single crystal silicon will show different absorption and refraction rate when laser irradiation with different wavelengths is applied. A single quantity called the complex refractive index can be used to define the different absorption and refraction of a medium.

$$\tilde{n} = n + i\kappa \tag{1}$$

The real part n is the refractive index and the imaginary part κ is the extinction coefficient. The absorption coefficient α is defined as:

$$\alpha = \frac{4\pi\kappa}{\lambda} \tag{2}$$

Secondly, the resonant frequencies of two different modes are obtained according to the temperature distribution of the resonator. The support of the disk resonator which is connected to the substrate is set as 273 K. The temperature of the disk resonator will increase when the laser power is irradiated on the surface, thus the resonant frequency decreases due to the decrease of the Equivalent stiffness. The formula of resonant frequency f is as below.

$$f = \frac{k}{2\pi R}\sqrt{\frac{E}{\rho(1-\nu^2)}} \tag{3}$$

Where k is the dimensionless frequency parameter, R is the disk radius, E, ν and ρ are Young's modulus, Poisson's ratio and density of the disk material separately. Due to the anisotropy of the single crystal silicon, the Young's modulus is expressed as an elastic matrix related to

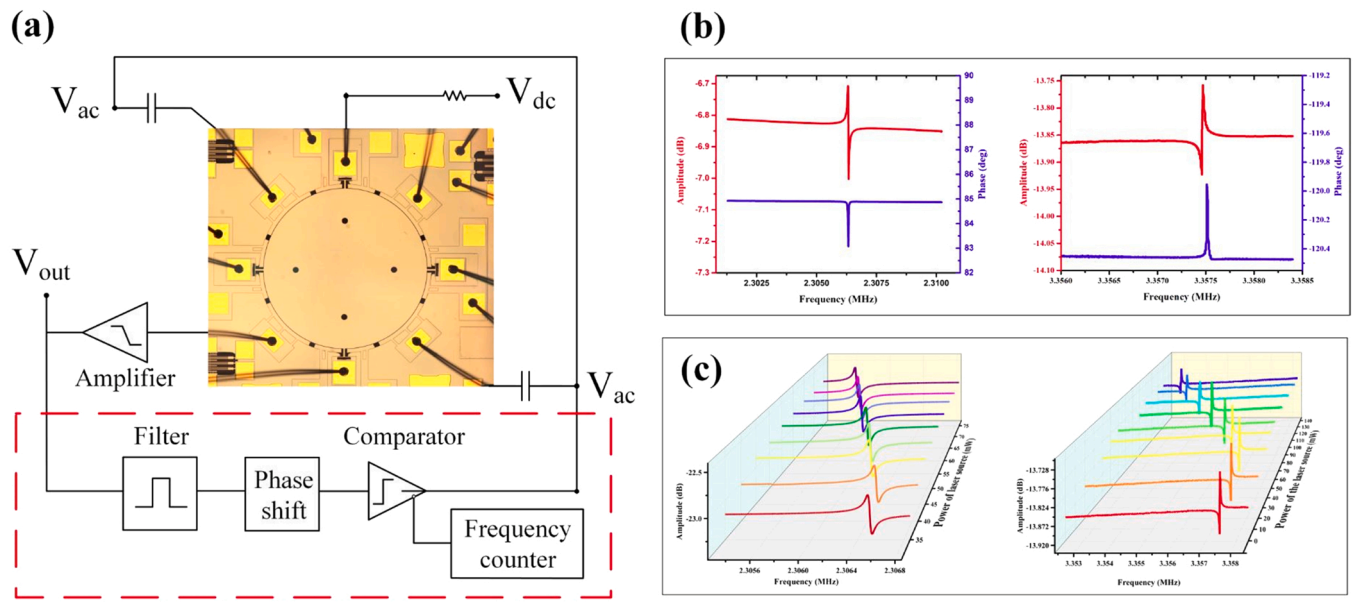

Fig. 2. (a) The schematic of the experiment. The circuit outside the red dotted rectangle is open-loop circuit. The closed-loop circuit is in the red dotted rectangle. (b) The amplitude and phase response of the elliptical mode (left) and contour mode (right) of SCS disk resonator without laser irradiation. (c) Frequency fluctuations of elliptical mode (left) and contour mode (right) are recorded when the power irradiation is increased.

temperature.

The relationship between laser power and center temperature of the disk resonator can be obtained from simulation (Fig. 1(b)). It shows that the center temperature rises much higher when 488 nm laser is irradiated than 1550 nm laser with the same power irradiation, which indicates a better heat absorption performance of our disk resonator. Then the resonant frequency is simulated based on different temperature distributions. Fig. 1(c) shows the simulated the relationship between laser power irradiation and resonant frequency of the elliptical mode when the laser power irradiation rises from 10 mW to 40 mW, and Fig. 1 (d) shows the simulated the relationship between the laser power irradiation and resonant frequency of the contour mode when the laser power irradiation is raised from 10 mW to 40 mW. As we can see in the figure, the simulated frequency shift induced by 488 nm laser is higher than the 1550 nm laser due to a different heat absorption performance.

From the simulation results, we can get the conclusion that the resonant frequency of the SCS disk resonator is sensitive with the laser power theoretically. Both the frequency of the elliptical mode and contour mode shift linearly with the laser power increase. For 488 nm laser, we calculate the ratio between frequency shift and original resonant frequency df/f_0 for both modes. Results show that the scale factor between df/f_0 and laser power of the contour mode is slightly higher than it of the elliptical mode Fig. 1(e). Corresponding experiments are needed to prove the conclusion, which will be showed as follows.

3. Experiment results

The resonator is microfabricated based on the standard silicon on insulator (SOI) technology. After wire bonding, the device is placed in vacuum environment for the following test. In our experiment, the device temperature is changed by the laser power irradiated on the center of the disk. A vacuum feedthrough is set to connect the atmosphere and the vacuum system. Optical fibers used for the transmission of laser are 600 μm in diameter. The optical fiber inside the vacuum cavity is set around 5 mm to the disk resonator. Since the relative position between the optical fiber and disk resonator will affect experiment results, the set-up is left undisturbed once it is well aligned during the whole experiment process. The wavelength of the laser power mainly used in our experiment is 488 nm due to the higher heat absorption

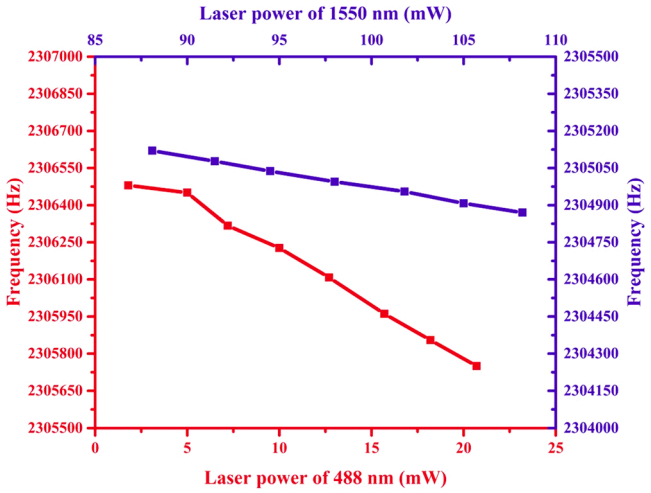

Fig. 3. Frequency shifts of the contour mode of the resonator under both 488 nm and 1550 nm laser irradiation.

performance. 1550 nm laser is also used in the open-loop experiment to prove the different heat absorption performance. Capacitive transduction is used to excite and detect the frequency response of the disk resonator, which is easy to conduct and will not be influenced by the increase of temperature. Electrostatic excitation with both a DC voltage and an AC voltage is applied on the disk resonator.

The schematic of the open-loop circuit is the part outside the red dotted rectangle in the schematic showed in Fig. 2(a). In the open-loop circuit method, an AC voltage is provided by a vector network analyzer. The resonant frequency of the elliptical mode and contour mode is firstly tested without the laser irradiation in the open-loop circuit (Fig. 2(b)). The resonant frequency from the experiment is quite close to results from the simulation. As the laser power increases in the experiment, temperature of the disk resonator will increase. Thus, the resonant frequency observed in the experiment decreases. Fig. 2(c) shows the frequency drifts of the elliptical mode and contour mode. The frequency shifts of the contour mode of the resonator are tested using 488 nm and

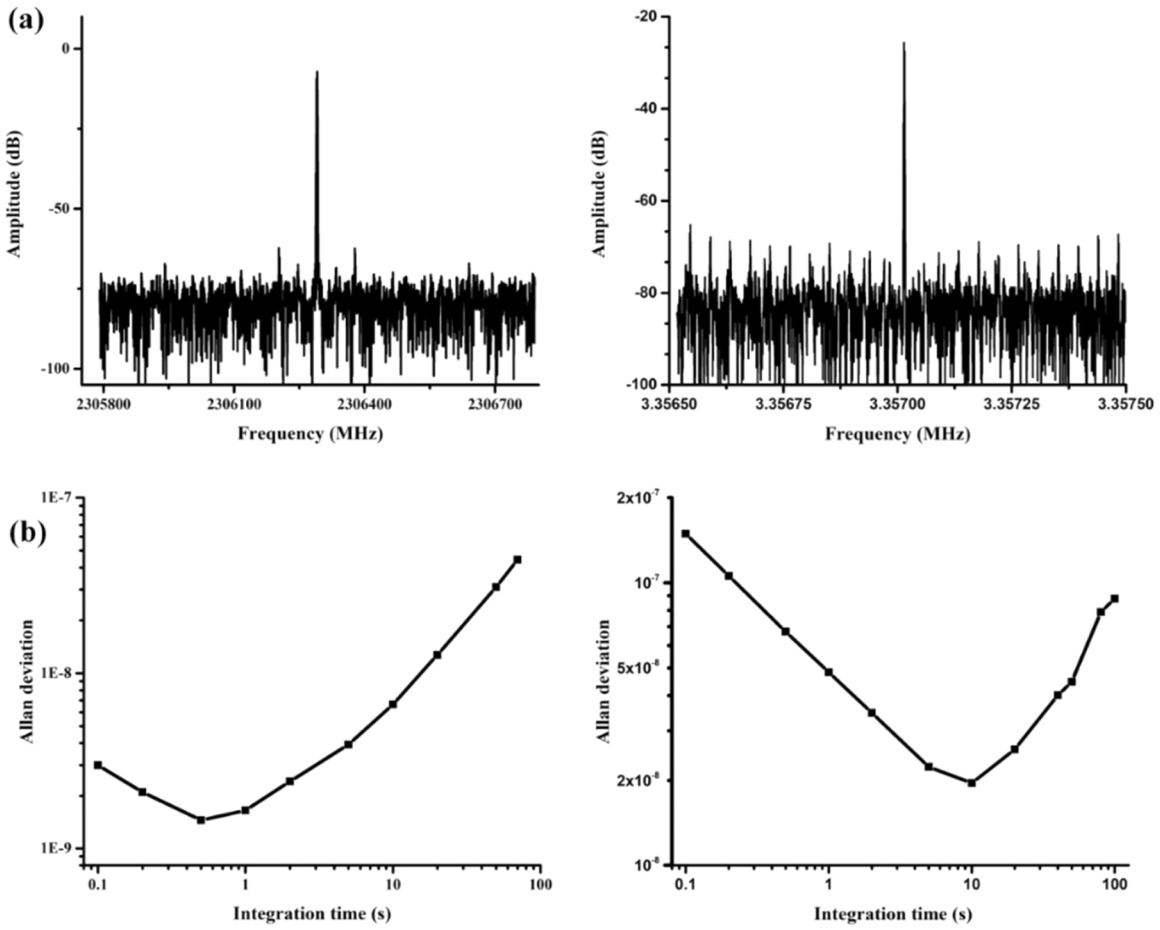

Fig. 4. (a) Frequency spectrum of elliptical mode (left) and contour mode (right) measured by a spectrum analyzer. (b) Allan deviation of the elliptical mode (left) and contour mode (right) of the disk resonator is calculated.

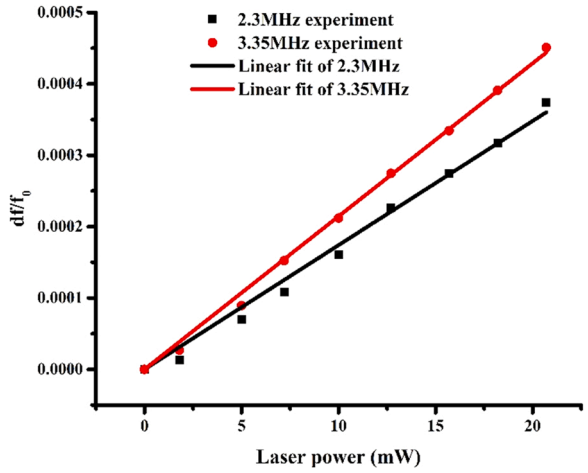

Fig. 5. The scale factor between df/f_0 and laser power of the contour and elliptical mode from experiment.

1550 nm laser irradiation (Fig. 3). It can be inferred from experiment results that the disk resonator is much more sensitive with 488 nm laser, which is consistent with the simulation. Therefore, performances of disk resonator under 488 nm laser irradiation will be the focus in the following text.

The schematic of the closed-loop circuit is showed in Fig. 2(a). The part of schematic in the red dotted rectangle shows the closed-loop circuit, which contains an amplifier, a filter, a phase shift and a comparator. In the closed-loop experiment, the AC voltage is provided by the comparator, the frequency response is measured by a spectrum analyzer, and the frequency outputs are recorded by a frequency counter. In the closed-loop testing, the frequency response of the elliptical mode (left) and contour mode (right) are measured by the spectrum analyzer is shown in Fig. 4(a).

Allan deviation is calculated with the frequency outputs recorded by the frequency counter to evaluate the stability of the elliptical mode and contour mode (Fig. 4(b)). The short-term frequency stability floor of the elliptical mode is 1.45ppb for an averaging time of 10 s, while the short-term frequency stability floor of the contour mode is 19.6ppb for an averaging time of 10 s

4. Performance parameters of the optical power meter

We calibrate the performance parameters of our optical power meter (for 488 nm) according to both open-loop and closed-loop experiment results. With the increasing of laser power of 488 nm irradiated on the resonator in the experiment, the elliptical mode and the contour mode show different scale factors between df/f_0 and laser power (Fig. 5). The difference of scale factors between two modes is verified by both simulation and experiment. This phenomenon may be related to several aspects. Firstly, when the laser power irradiates on the surface of disk resonator, thermal energy is decremented from the center. Since the mode shapes are different, a different heat distribution on the disk resonator will occur. Secondly, there is a heat flow on a vibrating disk even without external heating, since the temperature of compressed area

Table 1
Scale factor between df/f_0 and laser power of elliptical mode and contour mode in simulation and experiment.

Scale factor	Simulation	Experiment
Elliptical mode	6.19E-5	1.74E-5
Contour mode	6.67E-5	2.14E-5

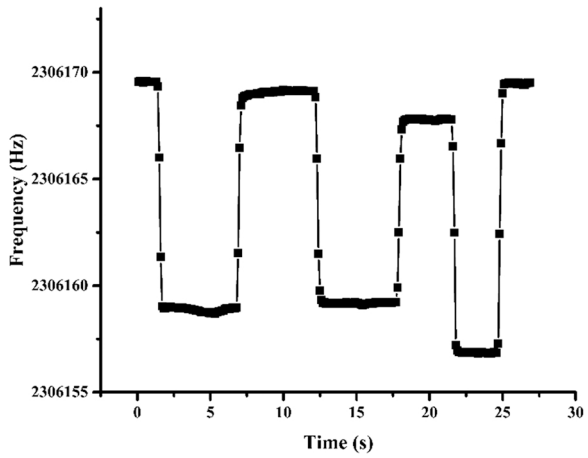

Fig. 6. The time sequence curve read by the frequency counter. The time interval between each dot is 0.1 s. The resonant frequency is back to stable in less than 0.3 s when the laser irradiation is changed.

of the disk is higher than the extended area. For different resonant modes, the energy damping is different, leading to a different mechanical loss [23].

The scale factor between df/f_0 and laser power of elliptical mode and the contour mode are listed in Table 1. According to Table 1, scale factor from simulation is much larger than the one from experiments. In our simulation, we set an ideal condition that all the laser power is absorbed by the disk resonator. However, the disk resonator used in our experiment is made of single crystal silicon. The reflection of laser and the thermal radiation of the disk resonator may be responsible for the low scale factor in the experiment. The gap in the absorptivity between the ideal value and the experiment value indicates that our optical power meter has potential in the improvement of absorptivity. More effective absorption materials attached on the disk resonator will be paid emphasis on in our future work.

The resolution of our optical power meter based on both elliptical mode and contour mode can be calculated by:

$$R = \frac{A \times f}{S} \tag{4}$$

Where A is the minimum Allan deviation, f is the resonant frequency of each mode and S is the scale factor between the frequency shift and laser power of the optical power meter based on each mode.

With the scale factor and the minimum Allan deviation of two modes, we can obtain that the resolution of the elliptical mode is 78 nW, while the resolution of the contour mode is 888 nW. Obviously, the resolution of elliptical mode is much higher than contour mode. Thus, elliptical mode is chosen as our detecting mode for our optical power meter. According to the experiment data in Fig. 5, the linearity of the elliptical mode is 99.924% calculated by Origin. Thus, our optical power meter has a good performance in linearity between the laser power and the frequency. To test the response time of our optical power meter in the closed-loop experiment, the power irradiation of the surface of our detector is increased from 0 mW to 0.245 mW, subsequently a laser power decrease about 0.23 mW is set. Then, two more cycles of heating (+0.225 mW, −0.2 mW, +0.25 mW, then return to zero) are applied to the disk resonator to prove the repeatability of the device. The time sequence curve showed by the frequency counter indicates that the frequency goes back to stable in about 0.3 s while the gate time is 100 ms (Fig. 6). Due to the delay time caused by the response of laser power and manual operation, the actual response time is less than 0.3 s. Faster response time can be reached by reduce the size of the disk resonator.

Since our optical power meter is a thermal detector, we believe it can be used for full waveband optical detection. However, when the target optical signal reach far infrared wavelength, the low absorption efficiency of silicon could limit the sensitivity of our optical power meter. Thus, efficient absorption layer for different target wavelength will be the focus of our future work. As a comparison, the performance of our optical power meter for 488 nm and different optical power meter is showed in Table 2.

5. Conclusion

The real-time optical power meter proposed in this work is based on a SCS micromechanical disk resonator, with a high resolution and linearity. The resonant frequency of resonator will fluctuate with the change of target laser power. Through comparative analysis on the performance of both elliptical mode and contour mode, we choose the elliptical mode as our working mode. The optical power meter proposed by us has the potential to detect full waveband laser power, and proper heat absorption layer for different laser wavelength will be the focus of our future work.

CRediT authorship contribution statement

X. Wei: conceived the concept, analyzed the data and wrote the manuscript. **X. Chen:** performed the experiments, analyzed the data and wrote the manuscript. **H. Wang** provided technical support and commented on the manuscript. All authors contributed through scientific discussions.

Table 2
Performance of different types of optical power meter.

Type	Performance	Main drawbacks	Reference
Photon detector	Spectral range: 3.1–8.9 μm	Need cooling equipment	[6]
Bimaterial microcantilever	Dynamic range: 1–300 pW Detection limit: less than 1 pW	Complexity of the sensor and read-out system	[14]
MEMS piezoelectric resonator	Dynamic range: 0.1 mW/mm^2 to 2.3 mW/mm^2. Linearity: $R^2 = 0.9954$ Response time: 0.7 ms	Complex read-out electronics are often needed due to high the resonant frequency to prevent strong electromagnetic interferences	[15]
Our detector	Dynamic range: Linearity: $R^2 = 0.99605$ Detection limit: 78 nW Response time: 0.3 s Spectral range: full waveband	Efficient absorption layer is required for different target wavelength, which will be the focus of our future work	This work

Declaration of Competing Interest

The authors declare that they have no known competing financial interests or personal relationships that could have appeared to influence the work reported in this paper.

Acknowledgements

This work is supported by the National Natural Science Foundation of China (52075432) and Program for Innovation Team of Shaanxi Province (2021TD-23). We also appreciate the support from International Joint Laboratory for Micro/Nano Manufacturing and Measurement Technologies.

References

[1] K. Setsuo, N. Yoshinobu, K. Kenji, K. Shunichi, A high-accuracy quick-response optical power sensor with μc-Ge:H thin film, Sens. Actuators A Phys. 28 (1) (1991) 63–68.
[2] R.G.W. Brown, R. Jones, J.G. Rarity, K.D. Ridley, Characterization of silicon avalanche photodiodes for photon correlation measurements. 2: active quenching, Appl. Opt. 26 (12) (1987) 2383.
[3] S. Cova, M. Ghioni, A. Lacaita, C. Samori, F. Zappa, Avalanche photodiodes and quenching circuits for single-photon detection, Appl. Opt. 35 (12) (1996) 1956–1976.
[4] P.G. Datskos, N.V. Lavrik, S. Rajic, Performance of uncooled microcantilever thermal detectors, Rev. Sci. Instrum. 75 (4) (2004) 1134–1148.
[5] Marion B. Reine, HgCdTe photodiodes for IR detection: a review. Photodetectors: Materials and Devices VI. Vol. 4288. International Society for Optics and Photonics, 2001.
[6] Y.F. Lao, A.G. Perera, L.H. Li, S.P. Khanna, E.H. Linfield, Y.H. Zhang, T.M. Wang, Mid-infrared photodetectors operating over an extended wavelength range up to 90 K, Opt. Lett. 41 (2) (2016) 285–288.
[7] M. Hammerich, A. Olafsson, A versatile, low-cost pyroelectric laser power monitor for the 1 mW to 50 W range, J. Phys. E Sci. Instrum. 21 (1) (1988) 80–83.
[8] J.G. Edwards, A standard calorimeter for pulsed lasers, J. Phys. E Sci. Instrum. 8 (8) (1975) 663–665.
[9] M.M. Birky, Calorimeter for laser energy measurements. Appl. Opt. 10 (1) (1971) 132–135.
[10] A. Rogalski, Infrared detectors: an overview, Infrared Phys. Technol. 43 (3–5) (2002) 187–210.
[11] M. Razeghi, Current status and future trends of infrared detectors, Opto-Electron. Rev. 1998 (3) (1998) 155–194.
[12] A. Graf, M. Arndt, M. Sauer, G. Gerlach, REVIEW ARTICLE:, review of micromachined thermopiles for infrared detection, Meas. Sci. Technol. 18 (7) (2007) R59–R75.
[13] P.G. Datskos, N.V. Lavrik, S. Rajic, Performance of uncooled microcantilever thermal detectors, Rev. Sci. Instrum. 75 (4) (2004) 1134–1148.
[14] Carlo Canetta, Arvind Narayanaswamy, Sub-picowatt resolution calorimetry with a bi-material microcantilever sensor, Appl. Phys. Lett. 102 (10) (2013), 103112.
[15] H.T. Li, P. Skands, Resonant and resistive dual-mode uncooled infrared detectors toward expanded dynamic range and high linearity, Appl. Phys. Lett. 110 (26) (2017) 59–66.
[16] M. Raiszadeh, Gallium nitride micromechanical resonators for IR detection, Micro-Nanotechnol. Sens., Syst., Appl. IV Int. Soc. Opt. Photonics (2012) 3190–3196.
[17] M. Rinaldi, H. Yu, C. Zuniga et al. High frequency AlN MEMS resonators with integrated nano hot plate for temperature controlled operation, 2012, pp. 1–5.
[18] F. Ferrieu, G. Auvert, Temperature evolutions in silicon induced by a scanned cw laser, pulsed laser, or an electron beam, 1983, 54(5), pp. 2646–2649.
[19] Z. Qian, S. Kang, V. Rajaram, et al., Narrowband MEMS resonant infrared detectors based on ultrathin perfect plasmonic absorbers, Sens. IEEE (2017) 1–3.
[20] S. Ogawa, K. Okada, N. Fukushima, M. Kimata, Wavelength selective uncooled infrared sensor by plasmonics, Appl. Phys. Lett. 100 (2) (2012) 113–163.
[21] Z. Qian, Y. Hui, F. Liu et al. 245 MHz graphene-aluminum nitride nano plate resonator//Transducers & Eurosensors Xxvii: the, International Conference on Solid-State Sensors, Actuators and Microsystems, IEEE, 2013, pp. 2005–2008.
[22] Z. Qian, Y. Hui, F. Liu et al. Graphene–aluminum nitride NEMS resonant infrared detector, 2016, 2:16026.
[23] G. Cagnoli, M. Lorenzini, E. Cesarini, F. Piergiovanni, M. Granata, D. Heinert, F. Martelli, R. Nawrodt, A. Amato, Q. Cassar, J. Dickmann, S. Kroker, D. Lumaca, C. Malhaire, C.B. Rojas Hurtado, Mode-dependent mechanical losses in disc resonators, Phys. Lett. A 382 (33) (2018) 2165–2173.

Xuan Chen is now a Ph.D. candidate in the State Key Laboratory for Mechanical Manufacturing Systems Engineering, Xi'an Jiaotong University, China. Her research interests include resonant MEMS sensors and microfluidics.

Xueyong Wei received his M.S. degree in Xi'an Jiaotong University in 2005 and his Ph.D. degree in University of Birmingham in 2009. He then conducted the research on micromechanical inertial sensors in the University of Cambridge as a post-doctoral research associate. He joined the faculty of Mechanical Engineering Department at the Xi'an Jiaotong University in 2012, where he is presently a Professor in Microsystems Technology. His research interests include micromechanical resonators and oscillators, MEMS sensors, and Microfluidics. He won the FK Bannister Prize of University of Birmingham (2009), Young Scientist Award of Microsystem and Nanoengineering Summit (2017) and Shaanxi Science & Technology Award for Young Talents (2020). He serves as the Associate Editor of *IET Micro & Nano Letters*, Section Executive Editor-in-Chief of *Engineering*, an international journal launched by the Chinese Academy of Engineering in 2015. He has also served as session chair, organization chair of several home and international conferences.